Water in the lower crustal granulite xenoliths from Nushan, eastern China

Qun-Ke Xia, Xiao-Zhi Yang, Etienne Deloule, Ying-Ming Sheng, Yan-Tao Hao

Water in the lower crustal granulite xenoliths from Nushan, eastern China

Qun-Ke Xia,[1] Xiao-Zhi Yang,[1] Etienne Deloule,[2] Ying-Ming Sheng,[1] and Yan-Tao Hao[1]

[1] Nominally anhydrous clinopyroxene (cpx), orthopyroxene (opx), and plagioclase (pl) from 10 lower crustal granulite (two-pyroxene granulite and hypersthene granulite) xenoliths in Cenozoic basalts from the Nushan volcano, eastern China, have been analyzed for their hydrogen content by microscopic Fourier transform infrared spectroscopy (Micro-FTIR). The results demonstrate that hydrogen was incorporated in all these minerals in the manner of OH and that the content (H_2O weight) is up to 2360 ppm for cpx, 1170 ppm for opx, and 880 ppm for pl. On the basis of the water content of constitutive minerals and their proportions, whole rock water contents of the Nushan granulites were estimated to be 150–950 ppm. Estimated equilibrium temperatures of the Nushan granulites are in the range of 810–892°C, corresponding to the lowermost crust at Nushan (about 25–30 km). Therefore this study provides direct evidence that the lower continental crust, even the lowermost part devoid of hydrous minerals, can contain a certain amount of water in nominally anhydrous minerals.

Citation: Xia, Q.-K., X.-Z. Yang, E. Deloule, Y.-M. Sheng, and Y.-T. Hao (2006), Water in the lower crustal granulite xenoliths from Nushan, eastern China, *J. Geophys. Res.*, *111*, B11202, doi:10.1029/2006JB004296.

1. Introduction

[2] The lower continental crust is the place where the crust-mantle interaction through time could be recorded. Therefore the knowledge of the content and distribution of water in the lower crust is a prerequisite to understand the water budget of the Earth. It is widely accepted that the deep continental crust consists mainly of metamorphic rocks in the granulite facies, which are dominated by pyroxenes, feldspar, quartz, and garnet [*Rudnick and Fountain*, 1995]. These are typically nominally anhydrous minerals (NAMs), and the lower continental crust is thus commonly considered to be "dry" [*Yardley and Valley*, 1997]. Several models of element abundance of the lower continental crust have been proposed [*Rudnick and Gao*, 2003, and references therein], whereas none of them has examined the abundance of hydrogen.

[3] During the last 20 years, hydrous components in NAMs have been the subject of increasing study. Hydrogen, bonded to structural oxygen as OH and less commonly H_2O, is found in many NAMs with the contents (expressed as H_2O weight (wt)) ranging from several to thousands of ppm [*Bell and Rossman*, 1992a; *Rossman*, 1996; *Ingrin and Skogby*, 2000]. Many efforts on natural and synthesized samples have led to an increasing consensus that water in NAMs may be the most important hydrogen reservoir in the Earth's mantle. Logically, the question which must be asked is how many water is borne in the lower continental crust minerals?

[4] In this paper, we investigate the main mineral phases (cpx, opx, and pl) from ten granulite xenoliths from Cenozoic basalts of the Nushan volcano, eastern China, by microscopic Fourier transform infrared spectroscopy (Micro-FTIR). The results demonstrate that these NAMs commonly contain significant trace amount of water as OH.

2. Geological Background and Samples

[5] The general geology of the Nushan volcano, eastern China, has been described in several recent publications [*Xu et al.*, 1998; *Yu et al.*, 2003; *Huang et al.*, 2004]. Briefly, the Nushan volcano is an isolated eruption center located at the southern edge of the North China Block (Figure 1) and belongs to the Jiashan-Liuhe volcanic complex. The volcanism began during the Paleocene (∼65 Ma) and continued until the Quaternary (∼0.6 Ma), with an evolution from tholeiite to alkali basalts. The K-Ar age of the Nushan volcano is about 0.63 Ma. The lava is mainly alkali basanite, and hosts numerous xenoliths and megacrysts.

[6] Ten xenoliths collected in alkali basanite from Nushan are two-pyroxene granulites and hypersthene granulites. They are fresh and 5–15 cm in size. All samples are characterized by a foliated structure in hand specimens, which is due to tabular plagioclase crystals. These granulites are predominantly composed of cpx, opx, and pl with subordinate quartz, magnetite and Fe-Ti oxides. Amphibole and biotite, the most common hydrous phases in Archean granulite terrains, were not observed in these granulites. All samples show a fine-grained granoblastic texture in which

[1]Chinese Academy of Sciences Key Laboratory of Crust-Mantle Materials and Environments, School of Earth and Space Sciences, University of Science and Technology of China, Hefei, China.

[2]Centre de Recherches Pétrographiques et Géochimiques-Centre National de la Recherche Scientifique, Vandoeuvre-les-Nancy, France.
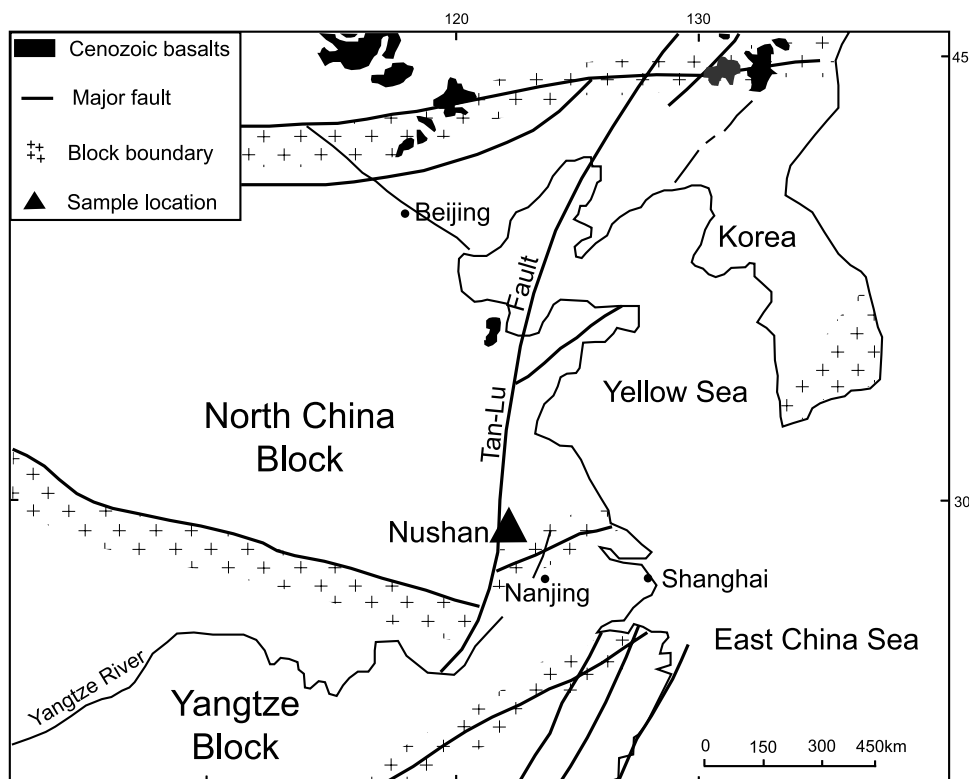
Figure 1. Location of the Nushan volcano in eastern China.

pyroxenes and plagioclases are usually 0.2–0.7 mm in size. The main petrographic and mineralogical characteristics of the samples are summarized in Table 1. Zircon U-Pb dating [*Huang et al.*, 2004] demonstrated that the protoliths of the Nushan granulites were most likely formed at ~2.5 Ga, metamorphosed at ~1.9 Ga, and disturbed by Mesozoic (~140 Ma) basaltic underplating.

3. Analytical Methods

[7] The chemical compositions of mineral phases were determined by electron microprobe (EMP) at the Micro-analysis Service Center at University of Nancy I, France. A Cameca SX50 EMP was used with 15 kV accelerating voltage, 20 nA beam current, <5 μm beam size, natural minerals and synthetic oxides as standards, and a program based on Pouchou and Pichoir procedure for data correction. Each mineral was analyzed for at least three points within the same thin section; the results show homogeneity. The average values are listed in Table 2.

[8] Double-polished thin sections with a thickness of 0.2–0.4 mm were used for the Micro-FTIR analysis. Infrared spectra were obtained at wave number between 570 and 7500 cm^{-1} using a Brucker Equinox 55 FTIR spectrometer coupled with a Hyperion 2000 microscope at Tongji University, China, and a Nicolet 5700 FTIR spectrometer coupled with a Continuμm microscope at University of Science and Technology of China (USTC). Measurements were carried out with unpolarized radiation with an IR light source, a KBr beam splitter and an MCT-A detector at room temperature. For each spectrum with a 2 or 4 cm^{-1} resolution, 128 or 256 scans were accumulated.

Apertures of 35×35 μm or 50×50 μm were used for selecting analytical areas free of inclusions and cracks under the $150 \times$ IR microscope. In order to minimize the uncertainty from unpolarized light for these anisotropic minerals (cpx, opx, and pl), $10-15$ grains for each mineral in each sample were analyzed and the averaged value was used to represent water content in the corresponding mineral.

[9] Water content of cpx, opx and pl in the Nushan granulites were calculated by the Beer-Lambert law:

$$c = \frac{18.02A}{\rho t \varepsilon \gamma} 10^3,$$

where c is the content of hydrogen species (expressed as H_2O weight in this paper), 18.02 is the molecular weight of H_2O, A is the integral area (cm^{-1}) of the absorption bands, ρ is the density of the sample (g cm^{-3}), t is the thickness of the sample (cm), ε is the molar absorption coefficient (L (mol H_2O cm^2)$^{-1}$), and γ is the orientation factor discussed by *Paterson* [1982]. In this study, the integral absorption region was 2800–3700 cm^{-1}, and the integral molar absorption coefficients were 38,300 L (mol H_2O cm^2)$^{-1}$ for cpx and 80,600 L (mol H_2O cm^2)$^{-1}$ for opx from *Bell et al.* [1995], and 107,000 L (mol H_2O cm^2)$^{-1}$ for pl from *Johnson and Rossman* [2003]. As the thickness variation for each section is <10% for more than 30 points covering the whole section, the average value was used for the different grains in the same sample; and the orientation factor of 1/3 was applied for the unpolarized spectra [*Paterson*, 1982]. The density of Nushan minerals was calculated from the proportion and density of end-members [*Deer et al.*, 1992]:

Table 1. Structure, Texture, and Mineral Assemblage of the Nushan Granulite Xenoliths[a]

Sample	Rock	Description	Mineral Assemblage
04NS1	hypersthene-bearing granulite	banded, fine-grain granoblastic texture with triple junction	opx+pl+qz
04NS5	two-pyroxene granulite	banded, fine-grain granoblastic texture with triple junction	opx+cpx+pl
04NS8	two-pyroxene granulite	banded, fine-grain granoblastic texture, partially altered	opx+cpx+pl+qz
04NS9	two-pyroxene granulite	banded, fine-grain granoblastic texture with triple junction	opx+cpx+pl
04NS11	hypersthene-bearing granulite	banded, heteroblastic texture	opx+pl+qz
04NS12	two-pyroxene granulite	fine-grain texture with triple junction	opx+cpx+pl
04NS13	hypersthene-bearing granulite	banded, heteroblastic texture	opx+pl+qz
04NS14	hypersthene-bearing granulite	banded, fine-grain grainblastic texture	opx+pl+qz
04NS15	two-pyroxene granulite	banded, fine-grain granoblastic texture with triple junction	opx+cpx+pl+mt
04NS16	two-pyroxene granulite	banded, fine-grain granoblastic texture with triple junction	opx+cpx+pl+mt

[a]Abbreviations are opx, orthopyroxene; cpx, clinopyroxene; pl, plagioclase; qz, quartz; mt, magnetite.

Wo 2.98 g cm^{-3}, En 3.21 g cm^{-3}, Fs 3.96 g cm^{-3}, An 2.76 g cm^{-3}, Ab 2.55 g cm^{-3}, Or 2.63 g cm^{-3}. The calculated density ranges 3.24–3.39 g cm^{-3} for Nushan cpx (Wo$_{41.1-45.4}$En$_{30.9-38.4}$Fs$_{18.1-24.9}$), 3.50–3.65 g cm^{-3} for opx (Wo$_{0.9-1.4}$En$_{40.8-60.3}$Fs$_{38.6-58.1}$) and 2.64–2.67 g cm^{-3} for pl (An$_{30-41}$Ab$_{55-64}$Or$_{4-11}$). Because of the minor variation of the densities calculated on individual minerals (only a few percent), the mean value of 3.58 g cm^{-3} for opx, 3.29 g cm^{-3} for cpx, and 2.65 g cm^{-3} for pl were used in this paper. Baseline corrections were carried out with a spline fit method by points outside the OH-stretching region. The influence from some possible alteration products (i.e., the bands at ~3700 cm^{-1}, see section 4.3) was estimated by Gaussian curve fitting method. Although the contribution of this band to the total integrated area is minor, 1–5% for cpx and opx and 3–12% for pl, it was eliminated. Some spectra show weak absorption at ~3740 cm^{-1}, which was an artifact from the silicon carbide source in the Nicolet instrument (G. R. Rossman, personal communication, 2005), was

also estimated by Gaussian curve fitting method and eliminated. The weak absorption at ~3250 cm^{-1} in some spectra was likely produced by ice film on the detector caused by liquid nitrogen [*Aines and Rossman*, 1984], it contributes very little to the whole integral intensity (<2%). The main uncertainty of the calculated results comes from (1) using unpolarized light, (2) baseline correction, (3) applying the absorption coefficients from *Bell et al.* [1995] and *Johnson and Rossman* [2003] directly to Nushan minerals, and (4) thickness variation for different grains within the same section, and the overall uncertainty is estimated to be 30–50%. The average water contents are listed in Table 3.

4. Results

4.1. Chemical Composition

[10] The opx and cpx have Mg # (=Mg/(Mg+Fe), assuming all Fe as Fe^{2+}) values ranging from 0.41 to 0.61

Table 2. Chemical Compositions of Minerals in the Nushan Granulite Xenoliths[a]

Sample	Mineral	SiO$_2$	TiO$_2$	Al$_2$O$_3$	Cr$_2$O$_3$	FeO	MnO	MgO	CaO	Na$_2$O	K$_2$O	Total	Mg #	Wo(An)	En(Ab)	Fs(Or)	T, °C	Density, g/cm^3
NS1	opx	49.23	0.00	0.73	0.00	33.58	1.27	14.55	0.65	0.00	0.00	100.01	0.44	1.39	42.97	55.64		3.63
NS4	opx	50.60	0.05	1.24	0.00	28.49	0.51	19.07	0.55	0.00	0.00	100.51	0.54	1.12	53.80	45.08	842	3.55
	cpx	51.24	0.23	2.13	0.02	11.03	0.14	12.64	21.31	0.46	0.01	99.21	0.67	44.86	37.01	18.12	842	3.24
	pl	57.85	0.04	26.23	0.00	0.05	0.04	0.00	8.15	5.94	0.68	98.99		41.37	54.54	4.09		2.67
NS8	opx	48.95	0.12	0.77	0.00	34.65	1.33	13.64	0.51	0.00	0.00	99.96	0.41	1.09	40.78	58.13	812	3.65
	cpx	51.19	0.16	1.90	0.00	14.56	0.49	10.12	20.15	0.65	0.00	99.23	0.55	44.19	30.88	24.93	812	3.30
NS9	opx	50.54	0.01	0.85	0.00	27.21	1.37	19.25	0.45	0.00	0.00	99.68	0.56	0.92	55.26	43.82	892	3.55
	cpx	51.39	0.28	2.22	0.01	12.34	0.79	12.93	19.25	0.62	0.04	99.88	0.65	41.08	38.37	20.55	892	3.27
	pl	58.92	0.00	25.15	0.01	0.00	0.00	0.01	6.25	6.36	1.82	98.53		31.36	57.78	10.86		2.65
NS11	opx	51.47	0.04	0.91	0.00	26.32	1.29	19.87	0.61	0.01	0.03	100.53	0.57	1.24	56.65	42.11		3.53
	pl	59.02	0.00	24.99	0.00	0.16	0.00	0.04	7.17	6.49	1.21	99.09		35.19	57.71	7.09		2.66
NS12	opx	48.75	0.10	1.82	0.00	30.95	0.71	16.32	0.57	0.00	0.00	99.21	0.48	1.20	47.88	50.93	810	3.59
	cpx	49.22	0.21	3.32	0.00	12.87	0.14	10.86	20.92	0.54	0.00	98.07	0.60	45.40	32.80	21.80	810	3.27
NS13	opx	50.08	0.16	1.08	0.00	27.06	1.13	19.37	0.65	0.00	0.02	99.55	0.56	1.34	55.30	43.36		3.54
	pl	59.70	0.00	25.01	0.00	0.03	0.00	0.04	6.34	6.96	0.72	98.79		32.01	63.67	4.32		2.65
NS14	opx	51.22	0.13	1.41	0.00	24.31	0.69	21.28	0.53	0.04	0.02	99.62	0.61	1.07	60.28	38.64		3.50
NS15	opx	50.99	0.02	0.95	0.00	26.62	0.56	20.03	0.56	0.03	0.00	99.76	0.57	1.14	56.63	42.23	860	3.53
	cpx	51.51	0.16	2.07	0.00	12.30	0.33	12.78	20.58	0.71	0.00	100.44	0.65	42.92	37.07	20.01	860	3.29
	pl	60.26	0.05	23.97	0.00	0.05	0.08	0.02	5.96	6.85	1.27	98.51		29.99	62.40	7.61		2.65
NS16	opx	50.50	0.01	0.64	0.00	28.00	2.35	18.47	0.63	0.00	0.00	100.59	0.54	1.30	53.33	45.37	849	3.56
	cpx	50.74	0.24	1.93	0.00	13.29	0.69	11.56	18.96	1.10	0.03	98.54	0.61	41.74	35.42	22.84	849	3.39
	pl	59.19	0.09	24.32	0.00	0.18	0.00	0.02	6.17	8.21	1.37	99.55		32.82	59.72	7.47		2.64

[a]Compositions are in wt %. T is calculated by the two-pyroxene geothermometer of *Wood and Banno* [1973]; the density of Nushan minerals is calculated from the proportion and density of end-members [*Deer et al.*, 1992]: Wo 2.98 g cm^{-3}, En 3.21 g cm^{-3}, Fs 3.96 g cm^{-3}, An 2.76 g cm^{-3}, Ab 2.55 g cm^{-3}, Or 2.63 g cm^{-3}; Mg # (= Mg/(Mg+Fe)), assuming all Fe as Fe^{2+}. Ab, albite; An, anorthite; En, enstatite; Fs, ferrosilite; Or, orthoclase; Wo, wollastonite.

Table 3. Water Contents in Minerals and Whole Rocks of the Nushan Granulite Xenoliths[a]

Sample	Modes	Water Content, ppm			Bulk Content, ppm
		opx	cpx	pl	
04NS1	$opx_{10}pl_{85}qz_5$	270		450	430
04NS4	$opx_{25}cpx_{15}pl_{60}$	615	2360	700	950
04NS8	$opx_{10}cpx_5pl_{60}qz_{25}$	545	2060	690	770
04NS9	$opx_{10}cpx_{30}pl_{60}$	410	220	360	320
04NS11	$opx_{20}pl_{72}qz_8$	430		440	440
04NS12	$opx_{10}cpx_{10}pl_{80}$	150	200	140	150
04NS13	$opx_{15}pl_{80}qz_5$	130		280	250
04NS14	$opx_{10}pl_{83}qz_7$	1170		880	920
04NS15	$opx_5cpx_{10}pl_{82}mt_3$	505	1260	550	630
04NS16	$opx_{10}cpx_5pl_{80}mt_5$	485	2360	800	850

[a]Bulk contents are calculated by $\Sigma \rho_i v_i c_i / \Sigma \rho_i v_i$, where ρ_i, v_i, c_i are the estimated density, volume proportion, and water content for each mineral, respectively; the modes were estimated on two to three thin sections.

and 0.55 to 0.67, respectively; and the end-member compositions are $Wo_{0.9-1.4}En_{40.8-60.3}Fs_{38.6-58.1}$ and $Wo_{41.1-45.4}En_{30.9-38.4}Fs_{18.1-24.9}$, respectively (Figure 2). In the figure proposed by *Rietmejir* [1983], all the Nushan samples fall in the metamorphic field (Figure 3). End-member compositions of plagioclase are $An_{30-41}Ab_{55-64}Or_{4-11}$.

[11] Equilibrium temperatures of these granulite xenoliths are estimated using the two-pyroxene thermometer of *Wood and Banno* [1973]. The yielded values range between 810 and 892°C, which is consistent with previous studies [*Yu et al.*, 2003; *Huang et al.*, 2004]. On the basis of the proposed geotherm at Nushan [*Xu et al.*, 1998; *Huang et al.*, 2004], these temperatures corresponds to a depth of 25 to 30 km. Petrological, geochemical and geophysical data [*Zhang et al.*, 1988; *Xu et al.*, 1998; *Huang et al.*, 2004] have constrained the depth of crust-mantle boundary at Nushan to be about 31 km. Therefore our granulite xenoliths sample the base of the lower crust.

4.2. Characteristics of Spectra in the Near-IR Region

[12] In the near-IR region $4000-7000$ cm^{-1}, the three minerals (opx, cpx, and pl) display different absorption phenomena: all the opx have a broad band at ~5200 cm^{-1} (Figure 4, curve a), all the cpx have a broad band at ~4300 cm^{-1} (Figure 4, curve b), while plagioclases have no absorption in this region (Figure 4, curve c). The broad bands for cpx and opx could not be only the combination or overtone of the fundamental modes, and it is suggested that they result from the electronic absorption of Fe^{2+} as the crystal field bands of Fe^{2+} (H. Keppler, personal communication, 2004). The position and shape of these bands are similar to the results of *Burns* [1993] for the same minerals.

4.3. Hydrogen Speciation and Water Content
4.3.1. Orthopyroxene

[13] In the typical OH vibration region ($3000-3800$ cm^{-1}), opx display six absorption bands: (1) ~3695 cm^{-1}; (2) $3610-3590$ cm^{-1}; (3) ~3580 cm^{-1}; (4) $3520-3505$ cm^{-1} (5) $3430-3415$ cm^{-1}; and (6) ~3370 cm^{-1}. Not all these six bands appear simultaneously, but combination of three or four bands is common (Figure 5a). The latter five bands fall in the typical IR absorption range of OH in opx [*Skogby et al.*, 1990; *Rauch and Keppler*, 2002; *Mierdel and Keppler*, 2004; *Stalder*, 2004], whereas the

first one appears too high. A series of investigations [*Skogby et al.*, 1990; *Bell and Rossman*, 1992a, 1992b; *Rossman*, 1996; *Ingrin and Skogby*, 2000; *Johnson and Rossman*, 2003] indicated that the IR absorption bands of OH in NAMs are generally observed in the region of $3000-3650$ cm^{-1}, while the bands in hydrous minerals usually appear at wave number higher than 3650 cm^{-1} because of the differences in the strength of hydrogen band. Pyroxenes are frequently altered to hydrous silicates such as talc and amphibole, and IR spectroscopy is very sensitive to these hydrous alteration products. Even occurring as submicroscopic lamellae (<5 nm in thickness for amphibole), these hydrous phases can give rise to sharp bands around $3670-3700$ cm^{-1} [*Miller et al.*, 1987; *Ingrin et al.*, 1989; *Skogby and Rossman*, 1989; *Skogby et al.*, 1990]. From the above comparison, we suggest that the first band is possibly related to some alteration products which may exist in the submicroscopic cracks, and the latter five bands are induced by OH vibration.

[14] The OH contents range from 130 to 1170 ppm for the opx from our 10 samples (Table 3). Water and Al_2O_3 contents form a positive trend, except samples 04NS12 and 04NS13 (Figure 6). This trend is similar to the results of solubility experiments from *Rauch and Keppler* [2002]. *Peslier et al.* [2002] also found a similar correlation for orthopyroxenes in spinel-peridotites from Mexico and Simcoe (Washington). Such a correlation suggests that the substitution of $Al^{3+} + H^+$ for Si^{4+} is an important incorporation mechanism of hydrogen in orthopyroxene. The deviation of two samples 04NS12 and 04NS13 from the trend is possibly due to hydrogen loss during transport to the surface, as well as their formation in a water poor source.

4.3.2. Clinopyroxene

[15] The FTIR spectra of cpx are characterized by four bands in the OH absorption range of $3000-3800$ cm^{-1}: (1) ~3700 cm^{-1}; (2) ~3620 cm^{-1}; (3) ~3530 cm^{-1}; and (4) ~3430 cm^{-1} (Figure 5b). The latter three are typical IR absorption bands of OH in cpx [*Skogby et al.*, 1990; *Bell and Rossman*, 1992a; *Rossman*, 1996; *Ingrin and Skogby*, 2000; *Peslier et al.*, 2002]. As discussed in section 4.3.1, the first band is possibly related to submicroscopic hydrous alteration products.

[16] The calculated water contents are $200-2360$ ppm for cpx from six samples (Table 3). The reported correlations between H_2O and several elements (Al, Mg, Ca, Na, etc.)
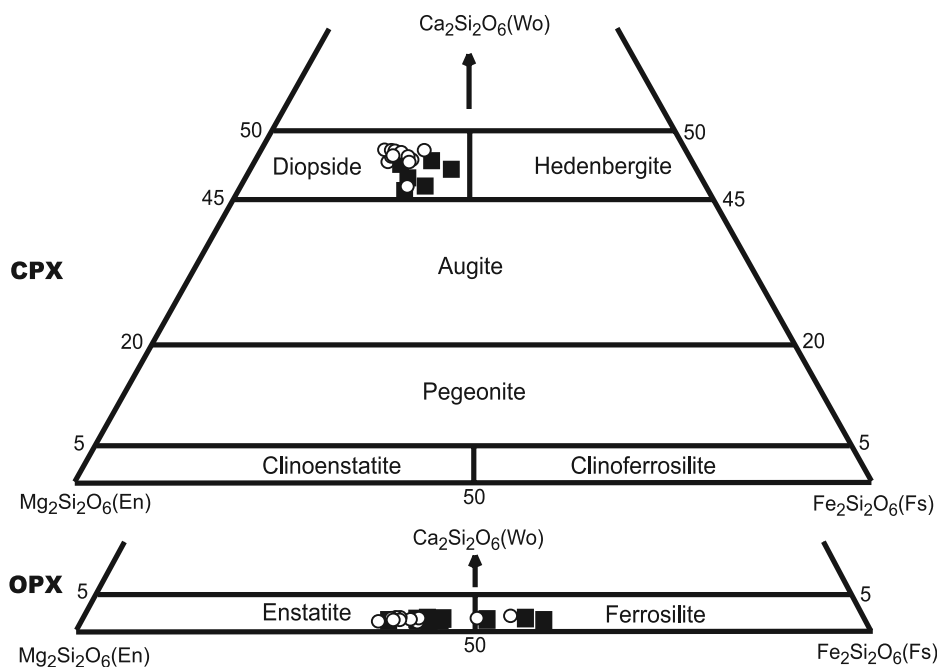
Figure 2. Compositional characteristics of clinopyroxene and orthopyroxene in the Nushan granulite xenoliths. Sources of data are solid square, this study, and open circle, *Huang et al.* [2004].

[*Skogby et al.*, 1990; *Smyth et al.*, 1991; *Peslier et al.*, 2002] were not observed in our samples.

4.3.3. Plagioclase

[17] In the wave number 3000–3800 cm^{-1} range, pl present complex IR absorption spectra, which can be approximately divided in five bands: (1) 3690–3710 cm^{-1}; (2) 3620–3630 cm^{-1}; (3) 3540–3565 cm^{-1}; (4) 3440–3470 cm^{-1}; and (5) 3400–3420 cm^{-1} (Figure 5c). *Johnson and Rossman* [2004] examined the IR spectra of 85 natural feldspars in a broad range of geological environments and summarized that absorption bands of

OH generally appear at 3050–3200 cm^{-1}, 3350–3450 cm^{-1}, $\sim$3500 cm^{-1}, and 3570–3610 cm^{-1}; and those of H$_2$O may occur at $\sim$3620 cm^{-1}, $\sim$3550 cm^{-1}, $\sim$3440 cm^{-1}, and $\sim$3280 cm^{-1}; the bands occurring at $\sim$3700 cm^{-1} are commonly due to alteration products such as sericite and clays. Because of small size (0.2–0.7 mm) and low water content of the Nushan granulite plagioclases, we cannot make sections thick enough for near−infrared (NIR) analysis to check whether the bands of the Nushan pl were from OH (the bending plus stretching combination band at $\sim$4550 cm^{-1}) or H$_2$O (the bending plus stretching combination band at
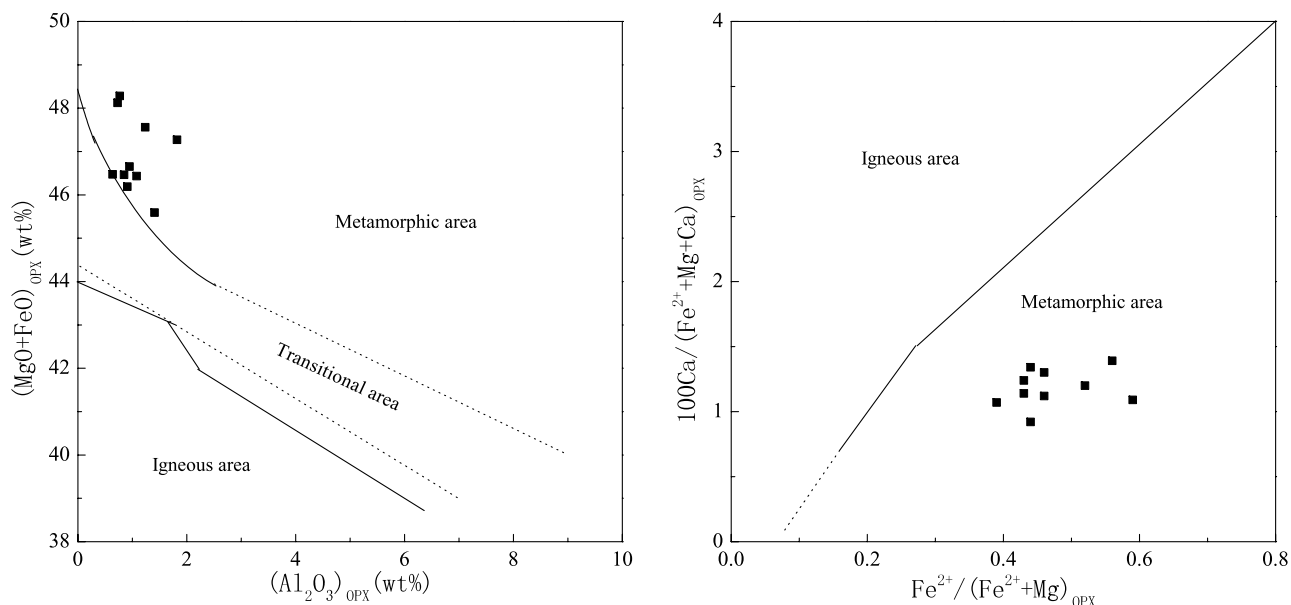

Figure 3. Petrogenetic discrimination diagrams of the orthopyroxenes in the Nushan granulites.
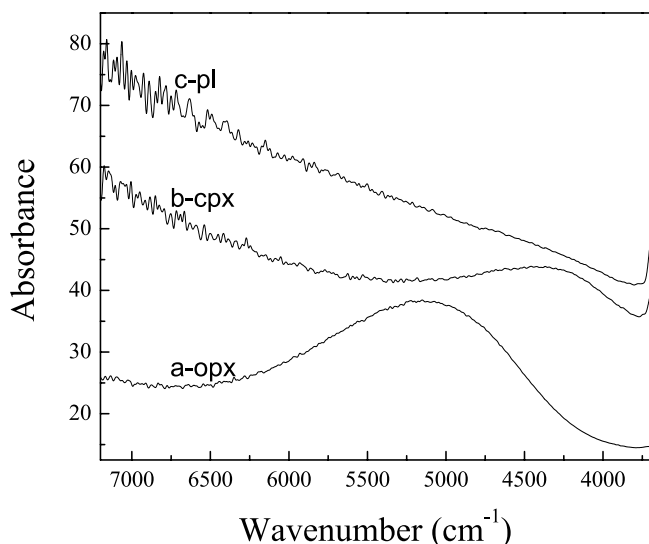
Figure 4. Representative spectra of orthopyroxene, clinopyroxene, and plagiocalse in near-IR region. All the spectra were normalized to 1 cm thickness but were vertically offset.

~5250 cm^{-1}). However, *Rossman* [1996] and *Johnson and Rossman* [2004] proposed that hydrogen in plagioclase is generally as OH whereas in alkali feldspar predominantly as H_2O. Therefore we ascribe the latter four bands in the Nushan plagioclases to OH. The calculated contents of water in the Nushan plagioclases are 140–880 ppm (Table 3). No correlation between H_2O content and major element contents can be found, similar to the study of *Johnson and Rossman* [2004].

4.4. Hydrogen Profile in Orthopyroxene

[18] In order to investigate the variation within individual grains, several large opx grains from different samples, which are clean and free of any visible inclusions and cracks, were selected for hydrogen profile analysis. The results did not reveal any zoning. Figure 7 shows a representative profile on an opx grain (~0.7 mm in size). A series of unpolarized FTIR spectra were collected at about 100 μm interval across the grain. The measured spectra show obvious absorption in the OH-stretching region with the bands at 3740 cm^{-1}, 3700 cm^{-1}, 3590 cm^{-1}, and 3420 cm^{-1}. The absorption at 3740 cm^{-1} is an artifact of the instrument and 3700 cm^{-1} is possibly from alteration products in submicroscopic cracks, while the other two bands are typical of OH in opx [*Skogby and Rossman*, 1989; *Skogby et al.*, 1990]. There is no significant difference between these spectra, as indicated by the integral absorption intensity (normalized to 1 cm^{-1}) displayed below each spectra in Figure 7. The very slight variations (<6%) are included in the uncertainty of background and baseline correction for each spectra. This suggests that the influence of hydrogen diffusion on initial water content in Nushan orthopyroxenes may be very minor.

5. Discussion

[19] It is debated whether or not the deep-seated minerals brought to the surface by alkali magma could preserve their initial water content. There are some geochemical evidences to support the retention of initial water content in natural NAMs [*Bell and Rossman*, 1992a; *Rossman*, 1996; *Matsyuk et al.*, 1998; *Peslier et al.*, 2002; *Bell et al.*, 2004], but hydrogen diffusion data suggest that the water content in NAMs may be modified during eruption, especially by reduction-oxidation reactions in iron-rich minerals [*Skogby and Rossman*, 1989; *Ingrin et al.*, 1995; *Wang et al.*, 1996; *Ingrin and Skogby*, 2000]. For our samples, it seems that most of opx can retain their original values based on the hydrogen profile measurements. Experimental data suggested that the diffusion rate of hydrogen in opx is in the same order of magnitude as that in diopside [*Ingrin et al.*, 1995; *Stalder and Skogby*, 2003] and faster than that in plagiocalse [*Johnson*, 2003]. Therefore Nushan cpx and pl should also have retained their initial water contents. However, hydrogen loss for some small grains cannot be ruled out, as suggested by the deviation of 04NS12 and 04NS13 from the positive trend between H_2O and Al_2O_3
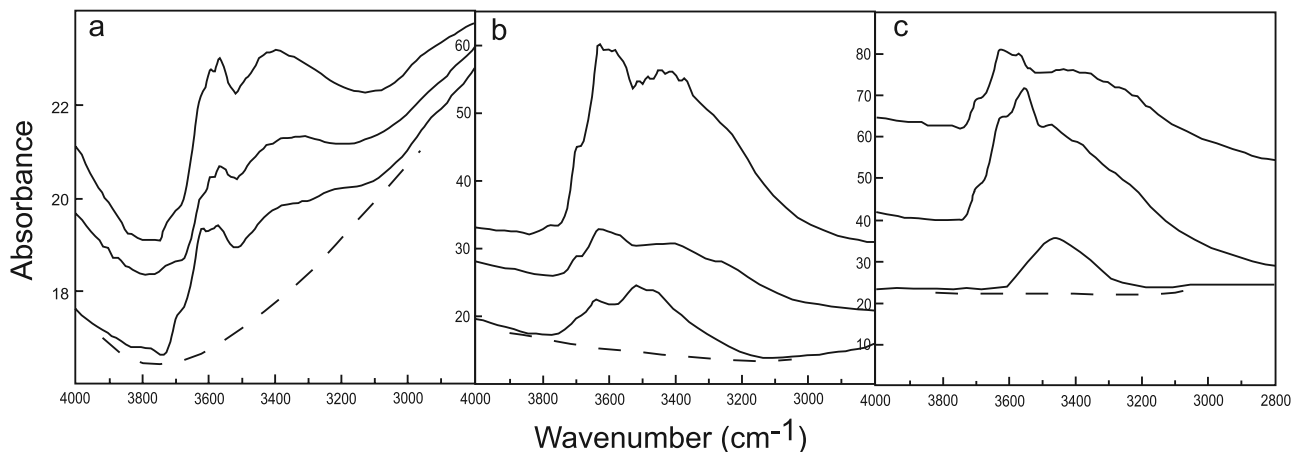

Figure 5. Representative IR spectra of minerals in the Nushan granulite xenoliths for (a) opx, (b) cpx, and (c) pl. Dotted lines correspond to the baseline used for the measurement of integral absorptions; all the spectra were normalized to 1 cm thickness but were vertically offset.
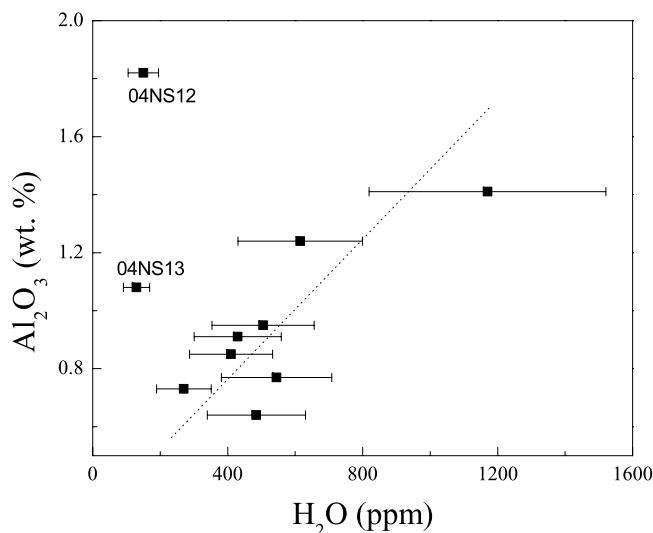
Figure 6. Correlation between H_2O (ppm wt) and Al_2O_3 (wt %) contents of the Nushan orthopyroxenes. Error bar indicates 30% of the H_2O content.

observed on the other orthopyroxenes (Figure 5). Therefore we have to bear in mind that the measured water contents may be the lower limit of the initial values.

[20] On the basis of the water contents, the volume proportions and the estimated densities of constitutive minerals, whole rock water contents of the Nushan granulites can be estimated to be 150 to 950 ppm (Table 3). These values are lower limits because the water from quartz,

magnetite and Fe-Ti oxides was not included. These minerals are, however, of minor proportions (<10%, except 04NS8 with 25% quartz) and a few analysis on quartz do not show OH absorption. Even if these whole rock water contents constitute a lower limit, our data confirm that the lower continental crust, even the lowermost part devoid of hydrous minerals, can contain significant amounts of structural water, ranging from 150 up to about 1000 ppm.

[21] Granulite is the main rock in the lower continental crust. Using an average water content of ~500 ppm for the lower crustal mafic granulite, and assuming that (1) the mass of the bulk continental crust is 2.44×10^{22} kg [*McLennan and Taylor*, 1999]; (2) the lower crust constitutes about 38.8% of the whole continental crust [*Rudnick and Fountain*, 1995; *Rudnick and Gao*, 2003]; and (3) the mafic granulites make up 70% of the lower crust [*Rudnick*, 1992; *Rudnick and Fountain*, 1995; *Rudnick and Gao*, 2003], the minimum amount of water stored in lower continental crust NAMs is about 3.31×10^{18} kg Hydrous minerals may also be an important phase in some regions (e.g., subduction zone) in the lowermost crust [*Rudnick and Fountain*, 1995] and contribute significantly to its water budget.

[22] Though the amount of water hosted by NAMs in the lower crustal granulites seems to be relatively small (approximately several hundred ppm, as exampled by Nushan samples), it is known that even a small amount of water can plays an important role in the geodynamics inside the Earth by changing the chemical and physical properties of many phases, including partial melting of rocks [e.g., *Gaetani et al.*, 1993; *Gaetani and Grove*, 1998; *Inoue*, 1994; *Hirose*, 1997; *Asimow and Langmuir*, 2003], diffusion [e.g., *Graham and Elphick*, 1991; *Wang et al.*, 2004], deformation
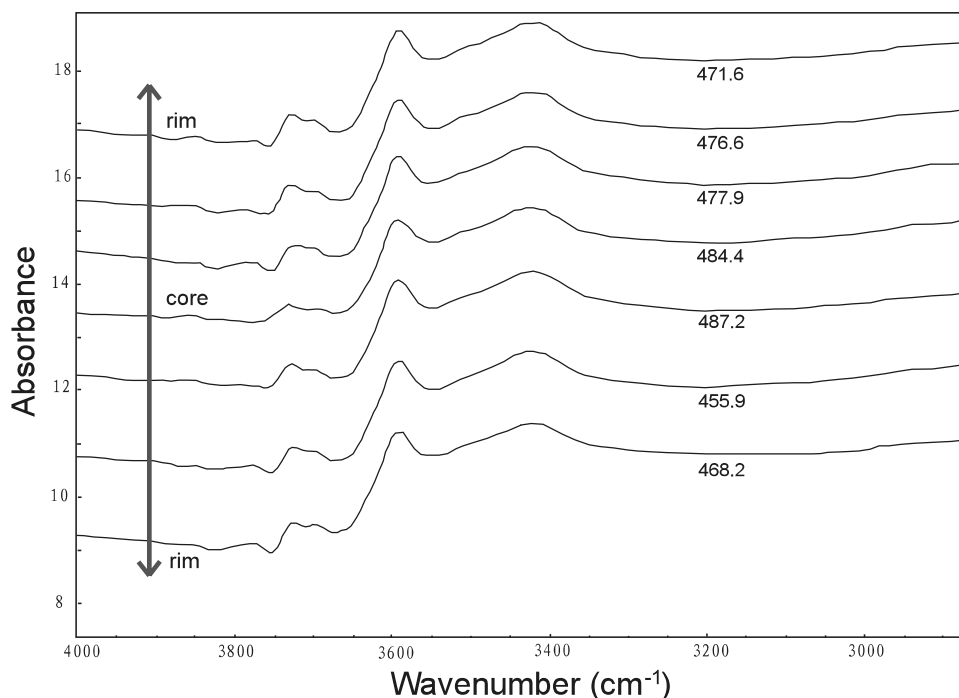

Figure 7. Hydrogen profile in an orthopyroxene grain from Nushan. The absorption at 3740 cm^{-1} is an artifact of the instrument and 3700 cm^{-1} is possibly from alteration products in submicroscopic cracks, while the other two bands are typical of OH in opx.

[e.g., *Mackwell et al.*, 1985; *Karato et al.*, 1986; *Mei and Kohlstedt*, 2000], viscosity [e.g., *Dixon et al.*, 2004], electrical conduction [e.g., *Karato*, 1990] or thermal conduction [*Hofmeister*, 2004]. Further study is needed to evaluate such effects of water in NAMs on the lower continental crust.

6. Conclusions

[23] Hydrogen, bonded to structural oxygen as OH, was found in nominally anhydrous orthopyroxene, clinopyroxene and plagioclase of the granulite xenoliths from Nushan volcano, eastern China. The contents (expressed as H_2O weight) is up to 1170 ppm, 2360 ppm, and 880 ppm, respectively, in the different phases. The whole rock water contents of the Nushan granulites can be estimated to range between ~150 and 950 ppm. This is the first study to demonstrate that the lower continental crust, even the lowermost part devoid of hydrous minerals, may contain a certain amount of water stored in NAMs. Further and more detailed investigations are needed to better describe its distribution in the lower crust and to understand the geochemical and geophysical role of water in granulites.

References

Aines, R. D., and G. R. Rossman (1984), Water in mineral? A peak in the infrared, *J. Geophys. Res.*, 89, 4059–4071.

Asimow, P. D., and C. H. Langmuir (2003), The importance of water to oceanic mantle melting regimes, *Nature*, 421, 815–820.

Bell, D. R., and G. R. Rossman (1992a), Water in Earth's mantle: The role of nominally anhydrous minerals, *Science*, 255, 1391–1397.

Bell, D. R., and G. R. Rossman (1992b), The distribution of hydroxyl in garnets from the subcontinental mantle of southern Africa, *Contrib. Mineral. Petrol.*, 111, 161–178.

Bell, D. R., P. D. Ihinger, and G. R. Rossman (1995), Quantitative analysis of hydroxyl in garnet and pyroxene, *Am. Mineral.*, 80, 465–474.

Bell, D. R., G. R. Rossman, and R. O. Moore (2004), Abundance and partitioning of OH in a high-pressure magmatic system: Megacryst from the Monastery Kimberlite, South Africa, *J. Petrol.*, 45(8), 1539–1564.

Burns, R. G. (1993), *Mineralogical Applications of Crystal Field Theory*, 2nd ed., Cambridge Univ. Press, New York.

Deer, W. A., R. A. Howie, and J. Zussan (1992), *An Introduction to the Rock-Forming Minerals*, 2nd ed., 696 pp., Pearson Educ., London.

Dixon, J. E., T. H. Dixon, D. R. Bell, and R. Malservisi (2004), Lateral variation in upper mantle viscosity: Role of water, *Earth planet. Sci. Lett.*, 222, 451–467.

Gaetani, G. A., and T. L. Grove (1998), The influence of water on melting of mantle peridotite, *Contrib. Mineral. Petrol.*, 131, 323–346.

Gaetani, G. A., T. L. Grove, and W. B. Bryan (1993), The influence of water on the petrogenesis of subduction related igneous rocks, *Nature*, 365, 332–334.

Graham, C. M., and S. C. Elphick (1991), Some experimental constraints on the role of hydrogen in oxygen and hydrogen diffusion and Al-Si interdiffusion in silicates, in *Diffusion, Atomic Ordering, and Mass Transport: Selected Topics in Geochemistry*, edited by J. Ganguly, *Adv. Phys. Geochem.*, 8, 248–285.

Hirose, K. (1997), Melting experiments on lherzolite KLB-1 under hydrous conditions and generation of high-magnesian andesitic melts, *Geology*, 25, 42–44.

Hofmeister, A. M. (2004), Enhancement of radiative transfer in the upper mantle by OH^- in minerals, *Phys. Earth planet. Inter.*, 146, 483–495.

Huang, X. L., Y. G. Xu, and D. Y. Liu (2004), Geochronology, petrology and geochemistry of the granulite xenoliths from Nushan, east China: Implications for a heterogeneous lower crust beneath the Sino-Korean Craton, *Geochim. Cosmochim. Acta*, 68, 127–149.

Ingrin, J., and H. Skogby (2000), Hydrogen in nominally anhydrous upper mantle minerals: Content levels and implications, *Eur. J. Mineral.*, 12, 543–570.

Ingrin, J., K. Latrous, J. C. Doukhan, and N. Doukhan (1989), Water in diopside: An electron microscopy and infrared spectroscopy study, *Eur. J. Mineral.*, 1, 327–341.

Ingrin, J., S. Hercule, and T. Charton (1995), Diffusion of hydrogen in diopside: Results of dehydration experiments, *J. Geophys. Res.*, 100, 15,489–15,499.

Inoue, T. (1994), Effect of water on melting phase relations and melt composition in the system Mg_2SiO_4-$MgSiO_3$-H_2O up to 15 GPa, *Phys. Earth planet. Inter.*, 85, 237–263.

Johnson, E. A. (2003), Hydrogen in nominally anhydrous crustal minerals, Ph. D. thesis, Calif. Inst. of Technol., Pasadena, Calif.

Johnson, E. A., and G. R. Rossman (2003), The content and speciation of hydrogen in feldspars using FTIR and 1H MAS NMR spectroscopy, *Am. Mineral.*, 88, 901–911.

Johnson, E. A., and G. R. Rossman (2004), A survey of hydrous species and contents in igneous feldspars, *Am. Mineral.*, 89, 586–600.

Karato, S. (1990), The role of hydrogen in the electrical conductivity of the upper mantle, *Nature*, 347, 272–273.

Karato, S., M. S. Paterson, and J. D. FitzGerald (1986), Rheology of synthetic olivine aggregates: Influence of grain size and water, *J. Geophys. Res.*, 91, 8151–8176.

Mackwell, S. J., D. L. Kohlstedt, and M. S. Paterson (1985), The role of water in the deformation of olivine single crystals, *J. Geophys. Res.*, 90, 11,319–11,333.

Matsyuk, S. S., K. Langer, and A. Hosch (1998), Hydroxyl defects in garnets from mantle xenoliths in kimberlites of the Siberian platform, *Contrib. Mineral. Petrol.*, 132, 163–179.

McLennan, S. M., and S. R. Taylor (1999), Earth's continental crust, in *Encyclopedia of Geochemistry*, edited by C. P. Marshall and R. W. Fairbridge, p. 712, Springer, New York.

Mei, S., and D. L. Kohlstedt (2000), Influence of water on plastic deformation of olivine aggregates: 1. Diffusion creep regime, *J. Geophys. Res.*, 105, 21,457–21,469.

Mierdel, K., and H. Keppler (2004), The temperature dependence of water solubility in enstatite, *Contrib. Mineral. Petrol.*, 148, 305–311.

Miller, G. H., G. R. Rossman, and G. E. Harlow (1987), The natural occurrence of hydroxide in olivine, *Phys. Chem. Mineral.*, 19, 1155–1164.

Paterson, M. S. (1982), The determination of hydroxyl by infrared absorption in quartz, silicate, glasses and similar minerals, *Bull. Mineral.*, 105, 20–29.

Peslier, A. H., J. F. Luhr, and J. Post (2002), Low water contents in pyroxenes from spinel-peridotites of the oxidized, sub-arc mantle wedge, *Earth planet. Sci. Lett.*, 201, 69–86.

Rauch, M., and H. Keppler (2002), Water solubility in orthopyroxene, *Contrib. Mineral. Petrol.*, 143, 525–536.

Rietmejir, F. M. J. (1983), Chemical distinction between igneous and metamorphic orthopyroxenes especially those coexisting with Ca-rich clinopyroxenes: A re-evaluation, *Mineral. Mag.*, 47, 143–151.

Rossman, G. R. (1996), Studies of OH in nominally anhydrous minerals, *Phys. Chem. Mineral.*, 23, 299–304.

Rudnick, R. L. (1992), Xenoliths—Samples of the lower continental crust, in *Continental Lower Crust*, edited by D. M. Fountain, R. Arculus, and R. W. Kay, pp. 269–316, Elsevier, New York.

Rudnick, R. L., and D. M. Fountain (1995), Nature and composition of the continental crust: A lower crustal perspective, *Rev. Geophys.*, 33(3), 267–309.

Rudnick, R. L., and S. Gao (2003), Composition of the continental crust, in *The Crust*, vol. 3, *Treatise on the Geochemistry*, edited by H. D. Holland and K. K. Turekian, pp. 1–64, Elsevier, New York.

Skogby, H., and G. R. Rossman (1989), OH^- in pyroxene: An experimental study of incorporation mechanisms and stability, *Am. Mineral.*, 74, 1059–1069.

Skogby, H., D. R. Bell, and G. R. Rossman (1990), Hydroxide in pyroxene: Variations in the natural environment, *Am. Mineral.*, 75, 764–774.

Smyth, J. R., D. R. Bell, and G. R. Rossman (1991), Incorporation of hydroxyl in upper-mantle clinopyroxenes, *Nature*, 351, 732–735.

Stalder, R. (2004), Influence of Fe, Cr and Al on hydrogen incorporation in orthopyroxene, *Eur. J. Mineral.*, 16, 703–711, doi:10.1127/0935-1221/2004/0016-0703.

Stalder, R., and H. Skogby (2003), Hydrogen diffusion in natural and synthetic orthopyroxene, *Phys. Chem. Miner.*, 30, 12–19.

Wang, L., Y. Zhang, and E. J. Essene (1996), Diffusion of the hydrous component in pyrope, *Am. Mineral.*, 81, 706–718.

Wang, Z., T. Hiraga, and D. L. Kohlstedt (2004), Effect of H^+ on Fe-Mg interdiffusion in olivine, $(Fe, Mg)_2SiO_4$, *Appl. Phys. Lett.*, 85, 209–211.

Wood, B. J., and S. Banno (1973), Garnet-orthopyroxene and orthopyroxene-clinopyroxene relationships in simple and complex systems, *Contrib. Mineral. Petrol.*, *46*, 1–15.

Xu, X. S., S. Y. O'Reilly, W. L. Griffin, X. M. Zhou, and X. L. Huang (1998), The nature of the Cenozoic lithosphere at Nushan, eastern China, in *Mantle Dynamics and plate Interactions in East Asia*, *Geodyn. Ser.*, vol. 27, edited by F. J. Flower, S. L. Chung, and C. H. Lo, pp. 167–196, AGU, Washington, D. C.

Yardley, B. W. D., and J. W. Valley (1997), The petrologic case for a dry lower crust, *J. Geophys. Res.*, *102*, 12,723–12,185.

Yu, J. H., X. S. Xu, S. Y. O'Reilly, W. L. Griffin, and M. Zhang (2003), Granulite xenoliths from Cenozoic basalts in SE China provide geochemical fingerprints to distinguish lower crust terranes from the North and South China tectonic blocks, *Lithos*, *67*, 77–102.

Zhang, S. W., S. X. Zhang, R. Y. Tang, Z. H. Liang, W. R. Song, J. M. Tang, J. D. Liu, and J. J. Song (1988), Interpretation of the Fuliji-Fengxian DSS profiles in Xiayangzi region (in Chinese with English abstract), *Acta Geophys. Sin.*, *31*, 367–648.

————————

E. Deloule, CRPG-CNRS, BP20, F-54501 Vandoeuvre-les-Nancy Cedex, France.

Y.-T. Hao, Y.-M. Sheng, Q.-K. Xia, and X.-Z. Yang, CAS Key Laboratory of Crust-Mantle Materials and Environments, School of Earth and Space Sciences, University of Science and Technology of China, Hefei 230026, China. (qkxia@ustc.edu.cn)